Reliability Analysis of Fatigue Crack Growth in Plain Concrete

Mustafa A. Aldalinsi
Misurata University / Department of Civil Engineering
Misurata, Libya
mustafa2280@yahoo.com

Abstract — **Civil engineers know that fatigue indicates the majority of structural failures. In plain and reinforced concrete structures, fatigue might account for excessive deformation, excessive of crack widths, de-bonding of reinforcement and rupture of the reinforcement, all of these can lead to structural collapse. Fatigue crack propagation can be a method to predict a remaining life of structures. Herein some works that have been done will be shown in order to analyse the fatigue crack growth for plain concrete specimens. The goals of this study are to estimate the critical crack length and remaining life of a plain concrete specimen, determine the state of the specimen either having failed or being safe using first order reliability method (FORM) and assess which parameter has most influence on the reliability index.**

Index Terms — **Fatigue, crack propagation, remaining life, first order reliability method (FORM).**

I. INTRODUCTION

In recent years, monitoring, repair, and renewal of Existing structures such as bridges and buildings have brought many challenges to civil engineers. The fatigue is a major cause of structural failure, so civil engineers should consider it carefully during a design stage. In plain and reinforced concrete structures, fatigue might account for excessive deformation, excessive crack widths, de-bonding of reinforcement and rupture of the reinforcement, all of these can lead to structural collapse, Perdikaris and Calomino, (1987). Fatigue crack propagation can be a method to predict a remaining life of a structure, so herein will show some works that have been done in order to analyze the fatigue crack growth for plain concrete. One of the most important efforts that have been made is how to predict the remaining life of structures based on variable amplitude of fatigue loads. This is done by proposing an improved fatigue crack propagation law that takes into account the loading history of a structure, frequency of the applied load, and the size effect parameters. According to linear elastic fracture mechanics concepts, a fatigue crack propagation law proposed by Slowik et al. (1996) is based on a variation of the Paris Law (1963), which is an empirical law characterizing fatigue growth for metals including parameters such as fracture toughness, loading history, and specimen size, except the frequency of externally applied load. Slowik et al. (1996) have been worked to adopt Paris Law (1963) to be adjusted for concrete. Therefore, they suggested that the fatigue crack propagation proposed law should be able to account for: 1) effect of loading history and sequence; 2) acceleration effect of spikes; and 3) size effect to be modeled for plain and reinforced concrete.

The concepts of fracture mechanics may be used as a mathematical tool for the assessment of residual strength and provide models that can be used to determine how cracks grow and how cracks affect the fracture strength of a structure. It is well known that the fatigue accounts for a bulk of material failures. Thus it is a well understood phenomenon for metallic structural components and causing untreatable material damage, Paris and Erdogan (1963). In case of concrete, the fatigue mechanisms are different from those in metals due to dissimilar fracture behavior.

A fracture process zone (FPZ) is a zone where the cement mortar matrix is intensively cracked. "Fracture of concrete is characterized by the presence of a fracture process zone at the crack tip," Sain and Kishen (2007) as shown in Figure (1). In the FPZ, there is no continuation for displacements while there is continuity in stresses. Thus, the stresses consider as a function of the crack opening displacement (COD). The tensile stress is equal to tensile strength of the material at the tip of the fracture process zone and it progressively decreases to zero at the tip of a true crack. It is assumed that in the very beginning the resulting damage occurs in the FPZ under low-cycle fatigue loading due to decrease in load-carrying capacity and stiffness, and it does not occur in the undamaged material, Foreman et al. (1967). If the FPZ shows greater sensitivity to fatigue loading than the surrounding material, then the fatigue behavior can be considered to be dependent on loading history, Slowik et al. (1996).Moreover, the size, shape, and fatigue behavior of the fracture process zone are dependent on specimen size and geometry, Zhang et al. (2001). Therefore, loading history considers the most important factor in fatigue behavior of concrete and only a nonlinear fracture mechanics model can describe it. Hence, the modification of metals' fatigue growth law is necessary in order to estimate the fatigue strength in plain concrete.

Received 26 September 2014; revised 5 October 2014; accepted 15 October 2014.
Available online 16 October 2014.

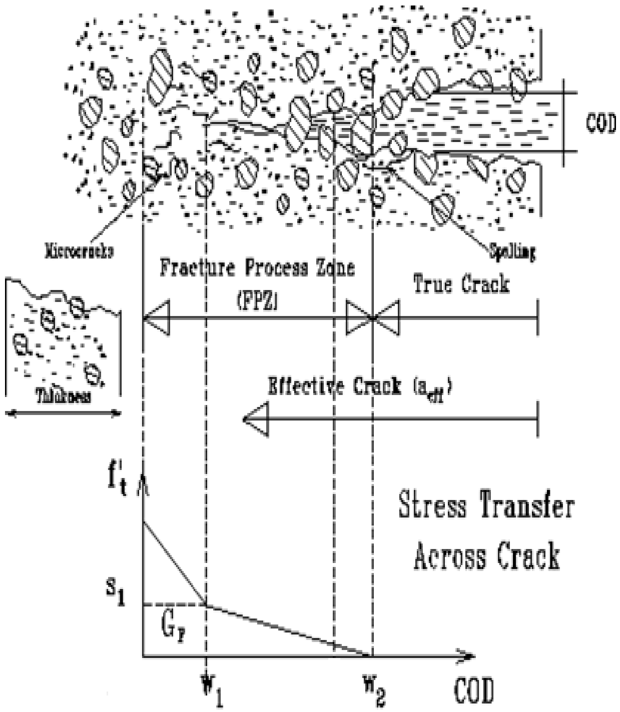

Figure 1. Fracture process zone, Sain and Kishen (2007)

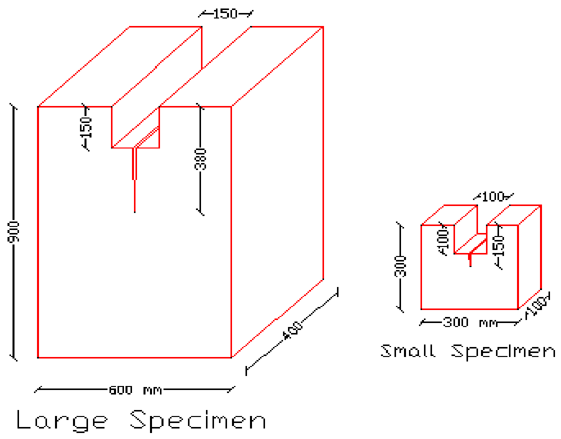

Figure 2. Specimens' dimensions

II. Proposed Model

In order to know how the proposed model, which is described later on and shown in equation (1), works based on the three laws Paris (1963), Farman (1967) and Walker (1970), it is important to show how the experiments were performed on wedge-splitting test specimens. The experiments were performed by Slowik et al. (1996). For the small specimens, a loading device was selected the same as the one introduced by Bruhwiler (1988) and Bruhwiler & Wittmann (1990). For large specimens, a loading device allows both crack opening and crack closure to be applied. The exact specimen dimensions are 914x610mm2 and 305x305mm2 (36x24 and 12x12 in2) sketched in figure (2).

Cracks were introduced during the test for the large specimens, while they were saw-cut for small ones. The concrete mixtures and material properties are shown in Table (1), Slowik et al. (1996). All specimens were cured in a fog room; small ones were tested at approximately 30 days and 90 days for the large specimens. Specific fracture energy was determined through identical wedge-splitting tests under monotonic, quasistatic loading, Saouma et al. (1991). Minor differences were noted between the small and large specimens, which can be marked to the difference in ligament lengths.

TABLE1. Concrete mix and material properties for small and large speicemns, Slowik et al. (1996).

	Small specimens	Large specimens
Cement, Type I	350 kg/m3	350 kg/m3
Water	182 l/m3	182 l/m3
Sand, 0 to 2.4 mm	761 kg/m3	761 kg/m3
Gravel, 2.4 to 12.5 mm	614 kg/m3	614 kg/m3
Gravel, 12.5 to 25 mm	538 kg/m3	538 kg/m3
Young's modulus Ec	16,000 Mpa	17,000 Mpa
Compressive strength fc'	30 Mpa	30 Mpa
Specific fracture energy GF	158 N/m	206 N/m
Fracture toughness K_{Ic}	0.95 MNm-3/2	1.48 MNm-3/2

III. Load Histories and Measurements

To simulate an earthquake loading in reality by keeping the number of test parameters to a minimum, a load system shown in figure (3) was selected. It is characterized by a basic sine vibrancy that is interrupted by spikes. This was obtained by a specially built programmable function generator connected to a standard controller. Load frequencies of 3 and 10 Hz were used. The applied load and the crack mouth opening displacements (CMOD) in the load line were recorded at sampling frequencies of 50 (for loading frequencies up to 3 Hz) to 200 Hz (for higher loading frequencies). The tests were run under load control. Tables (A) and (B) in the appendix summarize the load histories for small and large specimens, Slowik et al. (1996).

To determine the equivalent or effective crack length, a finite element calibration was performed for both specimen geometries. This was done through a linear elastic analysis for different crack lengths and for a constant value of the Young's modulus (E). A relation between the compliance and the effective crack length obtained from experiment result shown in tables (A) and (B) was determined in figure (4). During the test, a series of unload/reload cycles were performed. The specimens were unloaded down to 2% of the maximum load, and the compliance determined from the average slope of unloading and reloading branch. By comparing the initial compliance with the numerical one, the effective Young's modulus (E) was computed and in later comparisons the equivalent crack length was determined from figure (4), Slowik et al. (1996).

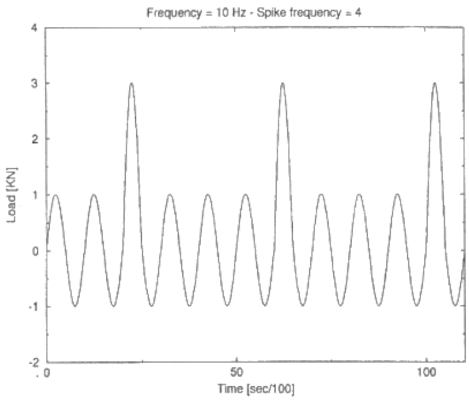

Figure3. Simulated earthquake loading applied in experiments, Slowik et al. (1996).

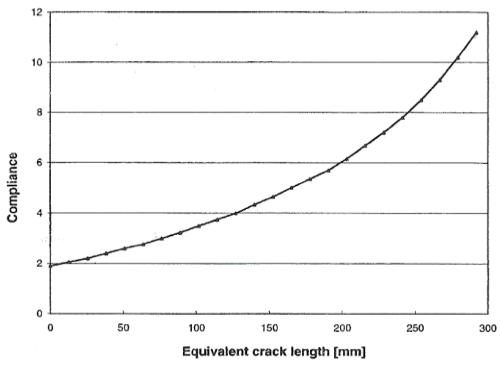

Figure 4. Compliance calibration curve for large specimens, Slowik et al. (1996).

IV. OPTIMIZED FATIGUE CRACK PROPAGATION MODEL FOR CONCRETE

Based on linear elastic fracture mechanics concepts, the fatigue crack propagation law proposed by Slowik et al. (1996) involves parameters such as fracture toughness, loading history, and specimen size, "except the frequency of externally applied load," Sain and Kishen (2007), and is described by

$$\frac{da}{dN} = C\left(\frac{K_{Imax}^{m}\Delta K_{I}^{n}}{(K_{IC} - K_{Isup})^{P}}\right) + F(a, \Delta\sigma) \qquad (1)$$

Where K_{Isup} represents the maximum stress intensity factor ever reached by the structure in its past loading history; K_{IC} represents the fracture toughness; K_{Imax} represents the maximum stress intensity factor in a cycle; ΔKI represents the stress intensity factor range; N is the number of load cycles; C is the crack growth rate per fatigue load cycle; and m, n, and P are constants. These constant coefficients are determined by, Slowik et al. (1996) using experimental data and they obtained 2.0, 1.1, and 0.7, respectively. Finally, the function F(a, Δσ) describes the effect of sudden overload onto the crack propagation.

A. Crack Growth Rate (C)

The parameter C in Equation (1) empirically gives a measure of crack growth rate per fatigue load cycle. This parameter in concrete members indicates the crack growth rate for a particular grade of concrete and is also size dependent. The value of C is determined by, Slowik et al. (1996) to be equal to 3.2x10-2 mm/cycle for small specimens and 9.5x10-3 mm/cycle for large ones. It should be observed herein that the stress intensity factor expressed in MNm-3/2. The C values were determined for a particular loading frequency of 3 Hz. Because parameter C gives an estimation of crack propagation rate in fatigue analysis, it should also depend upon the frequency of loading. Moreover, the fatigue crack propagation takes place primarily within the fracture process zone; thus, C should be related to the relative size of the fracture process zone, which is related to characteristic length. Therefore, C should depend on the characteristic length (lch) and ligament length (L), where lch=EGf/ft'2, and E is the elastic modulus of concrete, ft'2 is the tensile strength of the concrete, and Gf is the specific fracture energy. A linear relationship between parameter C and ratio of ligament length to characteristic length was proposed by Slowik et al. (1996) given by

$$C = \left(-2 + 25\,\frac{L}{lch}\right)x10^{-3}\,\frac{mm}{cycle} \qquad (2)$$

The equation (2) does not account for the frequency of fatigue loading. Hence, modification of this equation was proposed by Sain and Kishen (2007) including the effect of loading frequency. This was established through a regression analysis using the experimental results of Slowik et al. (1996), which have used compact tension specimens of two different sizes with loading frequency 3 Hz and interrupted by spikes. In a compact tension specimen, tensile force is applied in a direction perpendicular to the crack, thereby causing the propagation of the crack through the opening mode. The geometrical properties of these compact tension specimens are shown in Table (2). Also, the C values are reported by Slowik et al. (1996), which are computed by fitting the experimentally obtain a − N data into equation

(1) are shown in Table (3) along with the frequency of loading used in the test. The value of C times f (Cf) in terms of the ratio of ligament to characteristic length (L/lch) is given by

$$\mathrm{Cf} = -0.0193\left(\frac{L}{l_{ch}}\right)^2 + 0.0809\left(\frac{L}{l_{ch}}\right) + 0.0209\ \frac{mm}{second} \quad (3)$$

From equation (3), one can obtain the value of parameter C for any loading frequency, grade of concrete, and size of specimen.

TABLE 2. Geometry and material properties of specimens, Slowik et al. (1996)

Specimen	Depth, mm	Width, mm	Span, mm	Initial crack, mm	E, Mpa	KIC, MN/m3/2
Large	900	400	-	230	17,000	1.48
Small	300	100	-	50	16,000	0.95

TABLE 3. C values and material parameters, Slowik et al. (1996)

Lch	L/lch	GF N/m	C, mm/cycle	f. Hz	Cf, mm/s	Specimen size
238.74	1.38	206	32x10-3	3	0.096	Large
172	0.872	158	25.33x10-3	3	0.0285	Small

B. The Sudden Increase Function (F)

In concrete, the size of process zone is increased due to overload and the rate of crack propagation which is different in metals. In equation (1), the function F(a, Δσ) describes the sudden increase in equivalent crack length due to overload, Slowik et al. (1996). It should be observed herein that the function F is not related to fatigue directly but only takes care of the structural response due to overloads. Based on a nonlinear interpretation, overloads cause a sudden propagation of the fictitious crack tip, Slowik et al. (1996). The values of function F have been obtained for compact tension geometries by unloading and reloading at several load levels in the prepeak region and calculating the equivalent crack length from the corresponding compliances. Sain and Kishen (2007) developed a close form analytical expression to compute the sudden increase in crack length due to overloads. Since the rate of crack propagation due to overload depends on the nature property of concrete and stress amplitude, the function F was given by

$$F = \left(\frac{\Delta K_I}{K_{IC}}\right)\Delta a \quad (4)$$

Where ΔK_I indicates the instantaneous change in stress intensity factor from normal load cycle to a certain overload cycle which is given by Sain and Kishen (2007).

$$\Delta K_I = K_{overload} - K_{Inormal\ load} \quad (5)$$

Where $K_{overload}$ represents the maximum stress intensity factor due to overload, $K_{Inormal\ load}$ represents the maximum stress intensity factor due to normal load just before the overload. The value Δa is the increase in crack length with respect to its initial value before the application of overload and K_{IC} is the fracture toughness of concrete.

C. Strength Of Cracked Plain Concrete Beams

The basic equation that relates the stress intensity factor with applied load, specimen geometry, and crack size is given by Bazant and Kangming (1991).

$$K_I = \frac{Pf(\alpha)}{b\sqrt{d}} = \sigma_n\sqrt{d}\frac{f(\alpha)}{C_n} \quad (6)$$

Where α is the relative crack depth $\frac{a}{d}$, a is the crack length, d is the characteristic dimension of the structure such as depth of beam, b is the specimen thickness, P is the applied load, σn is magnitude of the applied nominal stress, and f(α) is a function depending on specimen geometry and for a three-point bend beam is given by.

$$f(\alpha) = (1-\alpha)^{-\frac{3}{2}}(1 - 2.5\alpha + 4.49\alpha^2 - 3.98\alpha^3 + 1.33\alpha^4) \quad (7)$$

The value C_n is a coefficient chosen for convenience to generalize the stress expression. For a three-point bend beam specimen having an initial notch length a_0, $C_n = \frac{3L}{\{2(d-a_0)\}}$.

V. Application to Compute Residual Life (KI) and Critical Crack Length (DA) of Plain Concrete

The model for computing the effective crack length (da) with the respect to the number of cycles of fatigue load, explained by equations (1) and (4), is used to come up with the number of load cycles required for dominant crack to reach a critical size. Moreover, the strength at a specific crack length can be determined from equation (6). By using equations in the foregoing, one can assess the residual strength of a plain concrete specimen using the following steps, Sain and Kishen (2007).

1. The effective crack length (da) versus the number of load cycles (N) relationship for the large specimen (G05) is plotted in figure (5) for a given concrete member using equation (1), (3) through (7).
2. The strength of the member as a function of continuously increase crack length (a) is determined from equation (6).
3. Using the plot obtained from step 1and shown in figure (5) the number of load cycles (NC) required for the existing crack to become critical, at the point when the curve becomes asymptotic, is determined. At NC, using the result in step 2, the current strength of the specimen is determined, which gives the residual strength.

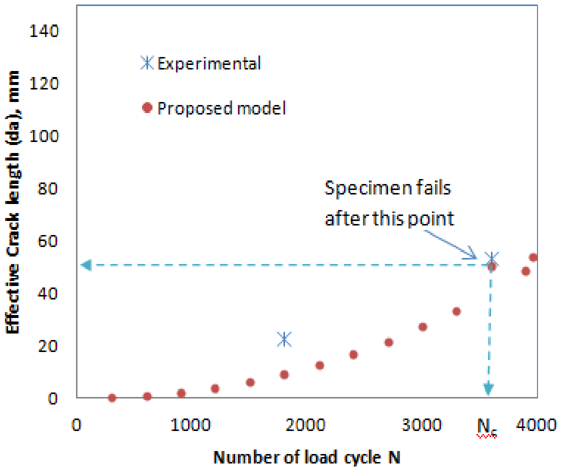

Figure 5. the effective crack length (da) vs. the number of load cycles (N) for the large specimen (G05).

A. *The Obtained Results From The Application*

1. The experiment results obtained by Slowik et al. (1996) and validated by Sain and Kishen (2007) for the large specimen (G05) were much closely the values plotted in figure (5).
2. The number of load cycle (Nc) required for the existing crack to become critical is equal to 3600.
3. The residual strength (KI) for the specimen (G05) is equal to $0.172\,\frac{\mathrm{MN}}{\mathrm{m}^{\frac{3}{2}}}$.
4. The critical crack length (da) before the specimen fail is equal to 50.64mm.

VI. Reliability Analysis

Structural reliability is defined as the probability that an item or facility will not perform its intended function for a specific period of time. Structural reliability theory and the principles of reliability analysis have been applied to many problems, such as design of structural components, control systems, and specific mechanical components. Classical reliability theory was developed to predict quantities such as the expected life and expected failure rate, given some tests or failure data for system and/or its components. Based on these predictions, the expected life and expected failure rate might be leading to required design life of a system.

Structural systems, in contrast to mechanical systems, do not tend to deteriorate, except by the mechanics of corrosion and fatigue, and in some cases might even get stronger, for instance: the strength of concrete increases with time and the strength of soil increases as a result of consolidation, but the problem is not lack of information for structural systems and their components regarding the time to failure, since they generally do not fail in service. The problem is of a different nature, Pendones (1991).

Structural systems and structural components fail when they meet an extreme load, or when a combination of loads causes an extreme load impact of considerable magnitude for a structure to reach failure state; this might be an ultimate or a serviceability condition. Therefore, the first consideration is to predict the magnitude of these extreme events, and the second is to predict the strength or load deflection characteristics of each structural component from the information available at the design stage. Likewise, it is important to come up with probabilistic models for the two parts of the problem which include first, all the uncertainties affecting the loading and second, all uncertainties affecting the strength or resistance of the structures, Thoft-Christensen and Baker (1982).

The goal of reliability analysis is to quantify how uncertainty in the parameters of the fatigue propagation law proposed by Slowik at el (1996) affects the prediction of the reliability. Knowing which parameter has more influence in the probability of failure of the structure and assessing which variables need extra research and attention, may help designers establish priorities for design stages.

A. *Reliability Analysis Of The Fatigue Crack Growth*

The limit state function used in this work is based on exceeding 50 mm of effective crack length, which is the length of which the large specimen (G05) fails. This happens when the number of load cycles is about 3600. It is assumed that the failure will occur if the length exceeds this specific length, and this is based on the obtained results from figure (5). The observation from the obtained results is that the effective crack lengths are growing when the number of load cycles increases from 300 load cycles to 3960 load cycles. At load cycle 3600 in particular, noting that the effective crack length is rapidly increasing because of a spike of loading from 50 kN to 62 kN. Therefore, there are sudden increases in maximum, range and history stress intensity factors, which are controlled by the second part of equation (1) or equation (4). This gives a clue that equation (4) has more influence than first part of equation (1) on fatigue crack growth.

The limit state function for exceeding the critical crack length is expressed as:

$$g = 50 - \left[C\left(\frac{K_{Imax}^{m}\,\Delta K_{I}^{n}}{(K_{IC} - K_{Isup})^{P}}\right) + \left(\frac{\Delta K_{I}}{K_{IC}}\right)\Delta a\right] * N \quad (8)$$

Where 50 mm is the assumed upper limit of the effective crack length of the large specimen (G05), N is the number of load cycle.

B. *Analysis Of Suggested Statistical Data*

Due to lack of statistical data, coefficient of variation (COV) equal to 0.1 for input parameters shown in table (4) was assumed for this study. Also, the assumption of using log-normal distribution for input parameters shown in table (4) was taken into account.

To check if the assumptions made are reasonable, Monte Carlo Simulation conducted for 1000 iterations.

The mean values of input parameters shown in table (4) were taken from table (1). Table (5) shows the mean values, standard deviations, and coefficients of variation of the effective crack lengths (da) obtained from Monte Carlo Simulation. These values were checked of using log-normal distribution in term of what is the best distribution fitting for them and that comes from the option of the best fit in Monte Carlo Simulation.

TABLE 4. Input parameters in equations (1) and (4)

Variable	Description
a_0	Initial crack length
a	Crack length
Pmin	Minimum applied load
Pmax	Maximum applied load
Psup	Maximum historical applied load ever reach
K_{IC}	Fracture toughness
C	Crack growth

TABLE 5.The values obtained from Monte Carlo Simulation

N	μda	Σda	COVda	2.5%	97.5%
300	0.260254	N/A	N/A	0	0
600	1.024586	1.7356	1.69	-2.16	4.84
900	2.305565	2.7029	1.17	-3.05	8.12
1200	4.118661	3.8688	0.94	-3.16	12.38
1500	6.482386	5.1782	0.8	-1.93	17.61
1800	9.418445	6.25	0.66	-1.7	22.6
2100	12.95192	7.8194	0.6	-0.11	29.68
2400	17.11144	9.3351	0.55	0.9	39.2
2700	21.92947	11.1336	0.51	2.9	46.7
3000	27.44248	12.7139	0.46	6.3	57.5
3300	33.6913	15.8606	0.47	8.7	70.2
3600	50.64579	23.4051	0.46	15.8	107.2
3900	48.88851	21.2772	0.44	15.8	105.6
3960	54.3848	23.3359	0.43	20.8	109.6

VII. Example Run Using COMREL-TI 8.10 Software and Assumed Data

To evaluate which output data has important effects on fatigue crack growth, the First Order Reliability Method (FORM) is used to estimate the probability of exceeding the limit state function described in equation (8) for a particular load cycle when N = 3000 cycles. The characteristics of the parameters used in the limit state function are listed in Table (4). Computations were done using Structural Reliability Software called COMREL – TI 8.10 developed by Reliability Consulting Programs (RCP). The statistical information shown in Table (5) for the input random parameters described in table (4) inserted in COMREL –TI 8.10 software. The results obtained from the software for this example are that the probability (Pf) of exceeding the limit state function (50 mm) described in equation (8) Pf = 4.95x10-2 which corresponds to reliability index, β =1.65 and sensitivity factors (α) are shown in figure (6).

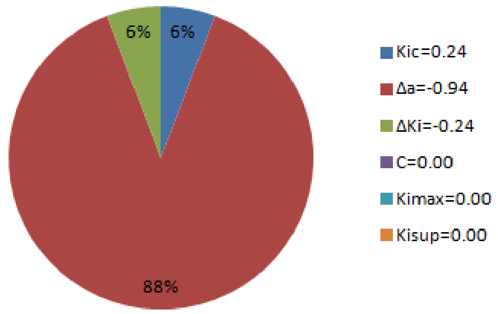

Figure 6. Importance factors

From the analysis of the sensitivity factors in this example, it is observed that the parameter (Δa) has the most influence on reliability index, the parameters KIC and ΔKI have very little influences, and the parameters KImax, KIsup, and C do not have any influences on reliability index.

TABLE 6.The parameters used in the sample runs

Variable	Description	Value
a_0	Initial crack length	230 mm
A	Crack length	330 mm
B	Specimen width	400 mm
D	Specimen depth	900 mm
Pmin	Minimum applied load	0 kN
Pmax	Maximum applied load	50 kN
Psup	Maximum historical applied load ever reach	75 kN
A	Relative crack depth	0.367
f(α)	Function of specimen geometry	1.021
K_{Imax}	Maximum stress intensity factor in a cycle	0.135 MN/m3/2
K_{Isup}	Maximum stress intensity factor ever reach in past specimen load history	0.202 MN/m3/2
K_{Iover}	Maximum stress intensity factor due to overload	0.135 MN/m3/2
$K_{Inormal}$	Maximum stress intensity factor due to normal load	0 MN/m3/2

ΔK_I	Stress intensity factor range	0.135 MN/m3/2
K_{IC}	Fracture toughness	1.48 MN/m3/2
C	Crack growth	3.2x10-2 mm/cycle
F	Function of sudden increase	9x10-3mm
Δa	Changing Length	100 mm
N	Number of load cycles	3000 cycle
m,n&p	Empirical constants	2,1.1&0.7

TABLE 7. Random variable used in the reliability analysis in the sample runs

Variable	Distribution	Coefficient of variation
Δa	Log-normal	0.4
K_{IC}	Log-normal	0.1
ΔK_I	Log-normal	0.1
C	Log-normal	0.1
K_{Imax}	Log-normal	0.1
K_{Isup}	Log-normal	0.1
M	Constant	-
N	Constant	-
P	Constant	-

VIII. CONCLUSION

In this study, statistical information is suggested for predicting the fatigue life of a plain concrete specimen considering fatigue crack propagation law proposed by Slowik et al. (1996). The output parameters which drive the fatigue process such as, crack growth rate, stress intensity factor range, fracture toughness, maximum stress intensity factor, and crack length range are considered as random variables. The reliability index is computed using COMREL-TI 8.1 software. It is seen from the case study that the reliability depends on crack length range, stress intensity factor range, and fracture toughness. Therefore, the fatigue crack propagation law needs to take into account the effect of both the initial crack length and the increment of crack length for accurate life prediction analysis of the plain concrete specimen.

A sensitivity analysis is performed to determine the predominant factor amongst the input parameters which influences the fatigue reliability prediction. It is observed that the reliability is more sensitive to the crack length range, followed by fracture toughness and stress intensity factor range. Beside this, the reliability computation was repeated for different values of coefficient of variation of the most sensitive factor, the crack length range, and other parameters are constant in term of coefficient of variation. The results show that the crack length range is the most influence parameter in most cases for safe fatigue life computations.

ACKNOWLEDGMENT

The author wish to thank Misurata University /Libya for giving such an opportunity for publication.

REFERENCES

[1] Anonymous. *Principle Guide for Service Life Planning of Buildings* (English Edition). *Architectural Institute of Japan*, Tokyo, Japan, (1993).
[2] Anderson, T.L. *Fracture Mechanics Fundamentals and Applications*, 3rd ed. Published by CRC Press, Taylor & Francis Group, 2005.
[3] Benjamin, J. R. and Cornell, C. A. *Probability Statistics and Decision for Civil Engineers*, McGraw-Hill Book Company, New York, N. Y.,1970, pp. 180-189.
[4] Bazant, Z. P., and Pfeiffer, P. A., "Determination of Fracture Energy from Size Effect and Brittleness Number," *ACI Material Journal*, V. 84, No. 6, pp. 463-480, November, 1987.
[5] Bruhwiler, E., "Fracture Mechanics of Dam Concrete Subjected to Quasistatic and Seismic Loading Conditions," Ph.D. dissertation, *No. 739*, Swiss Federal Institute of Technology, Lausanne. (in German), 1988.
[6] Bruhwiler, E., and Wittmann, F. H.,1990, "Wedge-Splitting Test: A Method of Performing Stable Fracture Mechanics Tests," *Engineering Fracture Mechanics*, 35.
[7] Bazant, Z., and Kangming, X., "Size Effect in Fatigue Fracture of Concrete," *ACI Material Journal*, V. 88, No. 4, pp. 427-437, July-August., 1991.
[8] Bazant, Z. P.; Xu, K., "Size Effect in Fatigue Fracture of Concrete," *ACI Material Journal*, V. 88, No. 4, pp. 390-399, July-August, 1991.
[9] British Standard (BSI), http://www.bsigroup.com/
[10] Chown, G. A.; Brown, W.C.; Kyle, B.R.; Lacasse, M.A.; and Vanier, D. J. "Applying Service Life and Asset Management Techniques to Roofing Systems," *National Research Council Canada*; Public Works and Government Service Canada, 1996.
[11] Choi, J.H., "The Fracture Analysis and Remaining Life Estimation of the AVLB Sub-Components," Master Thesis, Dept. Civil Eng., West Virginia University, 2000.
[12] http://wvuscholar.wvu.edu:8881//exlibris/dtl/d3_1/apache_media/5058.pdf
[13] Christios, G. P.; Petrou, M.F.; and Harries, K.A., "Fatigue Behavior of RC Beams Strengthened with GFRP Sheets," *Journal of Composites for Construction*, PP.246-253, November, 2001.
[14] Dowling, N. E., *Mechanical Behavior of Materials," Engineering Methods for Deformation, Fracture, and Fatigue*, Prentice Hall, Englewood Cliffs, New Jersey, 1993.
[15] Foreman, R.; Kearney, V.; and Engle, R., "Numerical Analysis of Crack Propagation in Cyclic-Loaded Structures," *Journal of Basic Engineering*, V. 89, pp. 459-464, 1967.
[16] Griffith, A.A., "The Phenomena of Rupture and Flow in Dolids," Philosophical Transactions, Series A, V. 221, pp. 163-198, 1920.
[17] Hongseob, O.; Sim, J.; and Meyer, .C. "Fatigue Life of Damage Bridge Deck Panels Strengthened with Carbon Fiber Sheets," *ACI Structural Journal*, V. 102, No. 1, pp. 85-92, January-February, 2005.
[18] Irwin, G.R., "Onset of Fast Crack Propagation in High Srength Steel and Aluminum Alloys," *Sagamore Research Conference Proceeding*. V. 2, pp. 289-305, 1956.
[19] Irwin, G. R., "Analysis of Stresses and Strains Near the End of a Crack Traversing a Plate", Transactions, ASME, *Journal of Applied Mechanics*, Vol. 24, 1957.
[20] International Standard http://www.iso.org/iso/iso_catalogue.htm International Union of Laboratories and Experts in Construction Materials, *Systems and Structures* (CIB / RILEM). www.rilem.net

[21] International Organization for Standardization (ISO). http://www.iso.org/

[22] Karbhari. V. M., "Rehabilitation and Renewal of Civil Structural Systems With Advanced Composites", ACCSE 1, *Advanced Composites in Civil and Structural Engineering Seminar*, University of Southern Queensland, Australia, 1998.

[23] [23Lounis, Z., Lacasse, M.A., Siemes, A. J. M. & Moser, K., "Further Steps Towards a Quantitative Approach to Durability Design." *Construction and the Environment-CIB World Building Congress*. Vol. 1, pp. 315-324, 1998.

[24] Liang, M.T.; Wang, K.L.; and Liang, C.H., "Service Life Prediction of Reinforced Concrete Structures," *Elsevier Science Ltd*, 1999.

[25] McGrath, P.F.; and Hooton, R.D., " Fick's Second Law," *Cement and Concrete Research*, V.26, No. 8, p. 1239, 1996.

[26] Moser, K. and Edvardsen, C., "Engineering Design Methods for Service Life Prediction," *EMPA Research & Testing Switzerland and COWI Consulting Engineers and Planners Denmark*, 2002.

[27] Paris, P. C., and Erdogan, F.,"A Critical Analysis of Crack Propagation Law," *Journal of Basic Engineering, American Society of Mechanical Engineers*, V. 85, No. 3, 1963.

[28] Perdikaris, P., and Calomino, A., "Kinetics of Crack Growth in Plain Concrete," *RILEM International Conference Fracture of Concrete and Rock, S. Shah and S. Swartz, eds.*, pp. 64-69, 1987.

[29] Perdikaris, P.C., and Calomino, A.M., "Kinetic of Crack Growth in Plain Concrete," *Proceedings of the International Conference on Fracture of Concrete and Rock, Houston*, pp. 96-101, June, 1987.

[30] Pendones, J. A., "Analysis of Uncertainties Related to the Response of Piers in Swelling Soils," *Master Thesis*, Dept. Civil Eng., University of Texas at El Paso, 1991.

[31] Swartz, S. E.; Jones, G. L.; and Hu, K., "Compliance Monitoring of Crack Growth in Concrete," *Journal of the Engineering Mechanics Division*, V. 104, No. 4, pp. 789-800, July-August, 1978.

[32] Saouma, V. E.; Broz, J. J; Bruhwiler, E.; and Boggs, H. L., " Effect of Aggregate and Specimen Size on Fracture Properties of Dam Concrete," *Journal of Material in Civil Engineering, American Society of Civil Engineering*, V. 3, No. 3, pp. 204-218, August 1991.

[33] Slowik, V.; Plizzari, G.; and Saouma, V., "Fracture of Concrete under Variable Amplitude Loading," *ACI Materials Journal*, V. 93, No. 3, pp. 272-283, May-June, 1996.

[34] Soronis, G., "Standards for Design Life of Buildings: utilization in the design process". *Construction and Building Material*, Vol. 10, No. 7, pp. 487-490, 1996.

[35] Sergio, F. B.; Benouaich, M. A.; Kreger, M.E.; Wood, S.L., "Fatigue Tests of Reinforced Concrete Beams Strengthened Using Carbon Fiber-Reinforced Polymer Composites," *ACI Structural Journal*, V. 102, No. 2, , pp. 305-314,March-April, 2005.

[36] Sain, T. and Kishen, C.J.M., "Prediction of Fatigue Strength in Plain and Reinforced Concrete Beams," *ACI Structural Journal*, V. 104, No. 5, pp. 621-628, September-October, 2007.

[37] Sain, T. and Kishen, C.J.M., "Probabilistic Assessment of Fatigue Crack Growth in Concrete," *International Journal of Fatigue*, V. 30, pp. 2156-2164,2008.

[38] Thoft-Christensen, P., and Baker, M. J., "Structural Reliability Theory and its Applications," *Springerverlang*, Berlin, 1982.

[39] Tang, L.P. and Nilsson, L.O., "Fick's Second Law," *ACI Mater Journal*, V. 89, No. 1, p. 49, 1992.

[40] The Canadian Standard, http://www.csa.ca/cm/ca/en/home

[41] *The Japanese Principal Guide*, http://www.jsa.or.jp/default_english.asp

[42] Vrouwenvelder, T., "The Joint Committee for Structural Safety". *TNO/TU*, Delft The Netherlands, 2001.

[43] Walker, E.K., "Effect of Stress Ratio during Crack Propagation and Fatigue for 2024-t3 and 7075-t6 Aluminum," Effects of Environment and Complex Load History on Fatigue Life, *American Society for Testing and Materials* STP 462, M. S. Rosenfeld, ed, pp. 1-14, 1970.

[44] Yang, Y.W., "A Study of Diffusion Behavior of Chloride Ion in High Strength Concrete," Master Thesis, Dept. Civil Emg., National Taiwan Ocean University, 1994.

[45] Zhap, Y. G. and Ono, T., "Moment Methods for Structural Reliability," *Structural Safety*. V. 23, pp. 47-75, 2001.

[46] Zhang, J.; Li, V. C.; and Stang, H., "Size Effect on Fatigue in Bending of concrete," *Journal of Material in Civil Engineering*, V. 13, No. 6, pp. 446-453, 2001.

BIOGRAPHY

Mustafa A. Aldalinsi was born in Misurata/Libya, on August 21, 1980. He received B.Sc. degree in Civil Engineering from University of Sirt at Hoon, in 2003. He got M. Sc. and Ph.D. degrees in Civil Engineering from the University of Texas at El Paso/USA in 2010 and 2013, respectively. Now, Mustafa is currently lecturer in Department of Civil Engineering at Misurata University/Libya. His research filed is applied in concrete testing and concrete materials.

APPENDIX

Table A. Loading histories and experimental results for small specimens, Slowik et al. (1996)

Loading Period	Specimen	K06	K08	K10	K12	K13	K14	K15	K17	K18
	Frequency, Hz	3	3	3	3	3	3	3	3	3
	Initial compliance, μm/kN	41.5	42.6	44.9	40.06	32	36.67	33.94	37.65	36.77
	Cycles	540	1*	1*	900	360	180	360	5000	1*
	Lower load, kN	0.55	0	0	0.2	1.1	0.2	0.2	0.5	0.5
1	Upper load, kN	1.65	2	1.5	1.2	2.1	1.2	1.5	1.5	2.6
	Spike, kN	—	2	1.5	—	—	—	—	—	2.6
	Equivalent crack, mm	0	13	14.7	0	2.5	0	0	1.3	14.2
	Cycles	900	100	180	900	540	720	540	5000	180
	Lower load, kN	0.55	1.4	0.9	0.5	1.1	0.2	0.2	0.5	0.5
2	Upper load, kN	1.65	2.45	2	1.5	2.1	1.2	1.5	1.5	2.1
	Spike, kN	—	—	—	—	—	—	—	—	—
	Equivalent crack, mm	1.3	Fail	16.7	1.3	3	0	2.8	1.3	15
	Cycles	1800		450	1*	360	900	360	1*	180
	Lower load, kN	0.55		0.9	0	0.8	0.5	0.5	1.5	0.5
3	Upper load, kN	1.65		2	1.5	1.8	1.5	1.8	2.6	2.1
	Spike, kN	—		—	1.5	—	—	—	2.6	—
	Equivalent crack, mm	1.8		Fail	1.8	3.6	0	3.8	51.3	16.5
	Cycles	1800			360	540	900	540	180	270
	Lower load, kN	0.55			0.8	0.8	0.8	0.5	0.3	0.5
4	Upper load, kN	1.65			1.8	1.8	1.8	1.8	0.85	2.1
	Spike, kN	—			—	—	—	—	—	—
	Equivalent crack, mm	1.8			3	4.8	2.8	5.1	51.8	18.8
	Cycles	3600			540	900	180	360	720	180
	Lower load, kN	0.55			0.8	0.5	1.1	0.8	0.3	0.5
5	Upper load, kN	1.65			1.8	1.5	2.1	2.1	0.85	2.1
	Spike, kN	—			—	—	—	—	—	—
	Equivalent crack, mm	1.8			3.6	4.8	3.6	11.4	52.1	19.3
	Cycles	1800			360	900	540	540	360	90
	Lower load, kN	0.55			1.1	0.2	1.1	0.8	0.6	0.5
6	Upper load, kN	1.65			2.1	1.2	2.1	2.1	1.15	2.1
	Spike, kN	—			—	—	—	—	—	—
	Equivalent crack, mm	2.3			9.1	5.6	3.8	13	58.9	20.8
	Cycles	1*			1*	360	360	180	540	30
	Lower load, kN	0			0	1.4	1.4	1.1	0.6	0.8
7	Upper load, kN	2.37			2.2	2.4	2.4	2.4	1.15	2.4
	Spike, kN	2.37			2.2	—	—	—	—	—
	Equivalent crack, mm	47.5			10.7	7.9	7.6	30.2	65.5	26.6
	Cycles	180			540	540	540	90	66	66
	Lower load, kN	0.31			1.1	1.4	1.4	1.1	0.9	0.8
8	Upper load, kN	1.12			2.1	2.4	2.4	2.4	1.45	2.4
	Spike, kN	—			—	—	—	—	—	—
	Equivalent crack, mm	52.1			11.4	9.4	10.9	36.6	75.9	33.8
	Cycles	900			360	540	540	27	10	15
	Lower load, kN	0.31			1.4	1.4	1.4	1.1	0.9	0.8
9	Upper load, kN	1.12			2.4	2.4	2.4	2.4	1.45	2.4
	Spike, kN	—			—	—	—	—	—	—
	Equivalent crack, mm	52.1			22.9	10.4	17	Fail	Fail	Fail
	Cycles	360			348	180	30			
	Lower load, kN	0.31			1.4	1.7	1.7			
10	Upper load, kN	1.12			2.4	2.7	2.7			
	Spike, kN	—			—	—				
	Equivalent crack, mm	66			Fail	16.3	Fail			

*Single spike

Table B. Loading histories and experimental results for large specimens, Slowik et al. (1996)

Loading Period	Specimen	G05	G06	G07	G08	G10	G11	G12	G13	G15
	Frequency, Hz	3	3	3	3	3	3	3	10	3
	Spike Frequency	5	5	5	5	5		5		5
	Initial compliance, μm/kN	1.99	1.8	2.04	1.84	1.97	1.96	1.8	1.89	1.79
1	Cycles	1800	900	900	900	180	900	15	900	900
	Lower load, kN	0	0	0	0	0	0	0	0	0
	Upper load, kN	50	50	50	50	50	50	50	50	50
	Spike, kN	—	—	—	—	—	—	—	—	—
	Equivalent crack, mm	22.9	8.4	8.2	8.4	1.5	3	nm	6.4	5.1
2	Cycles	1800	900	900	900	1620	2*	1*	900	900
	Lower load, kN	0	0	0	0	0	25	0	0	0
	Upper load, kN	50	50	50	50	50	70	125	50	50
	Spike, kN	62	—	—	75	—	70	125	—	—
	Equivalent crack, mm	53.3	8.9	10.2	34.3	2.5	3.6	nm	9.6	5.1
3	Cycles	360	900	900	45	1800	1*	3*	900	900
	Lower load, kN	25	25	25	25	-10	25	0	25	25
	Upper load, kN	75	75	75	75	50	117	50	75	75
	Spike, kN	—	—	—	—	—	117	—	—	—
	Equivalent crack, mm	Fail	27.9	34.3	nm	3.6	44.7	40.6	91.2	36.1
4	Cycles		900	900	90	180	1*	180	430	900
	Lower load, kN		25	25	25	25	25	0	25	25
	Upper load, kN		75	75	75	75	95	50	75	75
	Spike, kN		—	—	100	—	95	—	—	—
	Equivalent crack, mm		34.3	53.3	55.9	25.4	nm	43.2	Fail	42.7
5	Cycles		1*	540	45	720	1*	75		270
	Lower load, kN		0	60	25	25	25	0		60
	Upper load, kN		102	90	75	75	123	50		90
	Spike, kN		102	—	—	—	123	—		—
	Equivalent crack, mm		nm	76.2	nm	38.1	117	nm		117"
6	Cycles		540	180	90	900	900	7		
	Lower load, kN		60	60	25	0	0	0		
	Upper load, kN		90	90	75	50	50	50		
	Spike, kN		—	—	100	—	—	125		
	Equivalent crack, mm		76.2	nm	97.8	38.1	127	Fail		
7	Cycles		540	180	90	60	180			
	Lower load, kN		60	60	25	25	25			
	Upper load, kN		90	90	75	75	75			
	Spike, kN		—	97.2	—	—	—			
	Equivalent crack, mm		77.5	120.6	nm	nm	134.1			
8	Cycles		135	180	39	180	630			
	Lower load, kN		50	60	25	25	25			
	Upper load, kN		100	90	75	75	75			
	Spike, kN		—	—	110	92	—			
	Equivalent crack, mm		Fail	nm	Fail	53.85	Fail			
9	Cycles			5		60				
	Lower load, kN			60		25				
	Upper load, kN			90		75				
	Spike, kN			105		—				
	Equivalent crack, mm			Fail		nm				
10	Cycles					70				
	Lower load, kN					25				
	Upper load, kN					75				
	Spike, kN					110				
	Equivalent crack, mm					Fail				

*Single spike
"Failed during compliance measurement ˜Spike frequency=50, nm = not measured.